Calibration of a Parallel Robot Using Multiple Kinematic Closed Loops

Ali Nahvi, John M. Hollerbach

Biorobotics Laboratory
McGill University
3775 University St.
Montreal, Quebec H3A 2B4

Vincent Hayward

McGill Center for Intelligent Machines
McGill University
3480 University St.
Montreal, Quebec H3A 2A7

Abstract

A method is presented for autonomous kinematic calibration of a 3-DOF redundant parallel robot. Multiple closed loops are used in a least squares optimization method. Ill-conditioning, column scaling of the gradient matrix, and observability indices for the best pose set of robot calibration configurations are discussed. Experimental results are presented and compared with the results using an external calibration device.

1 Introduction

Recently, it has been shown that single-loop closed chains can be kinematically calibrated using joint angle readings alone [1]. By placement of the closed chain into a number of configurations, consistency conditions permit the kinematic parameters to be extracted.

Autonomous calibration is particularly useful for a number of reasons, nominal accuracy being only one of them. For example, in case of repair, replacement of a displacement sensor typically leaves the device uncalibrated since the origin may not be precisely known. With this technique, the device can regain its original accuracy without external calibration devices. Autonomous calibration is a technique to uphold nominal accuracy over extended periods of operation without maintenance.

A 6-DOF Hand Controller was recently calibrated by this approach using double closed loops [9]. In this paper a similar method is used to calibrate a shoulder joint's kinematic parameters. The parameters include sensor offsets and three other kinematic parameters.

Wampler and Arai also used kinematic closed loops to calibrate a three-leg planar parallel-link manipulator [16]. A laser tracking coordinate measuring machine was self-calibrated in [17]. Four trackers provided redundant sensing of the manipulator endpoint, and this redundant sensing was used to calibrate the relative locations of the trackers. Boulet applied closed-loop calibration to a mechanical two-loop system formed as a single joint with two antagonistic linear actuators which is a precursor to the present mechanism [3].

The mechanism used in the calibration experiments is a 3-DOF platform type closed-chain mechanism
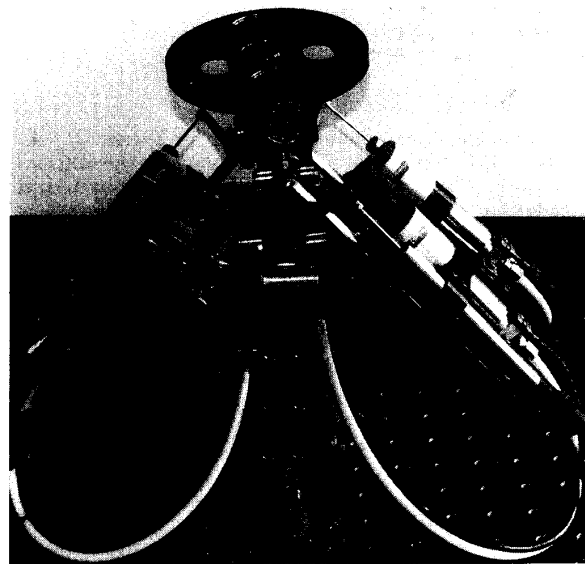

Figure 1: 3-DOF redundant shoulder joint.

with its output link constrained to undergo spherical motions (Figure 1). It is intended to form the shoulder joint for a complete manipulator with a hybrid kinematic design. Previous work on this chain includes kinematic modeling [7], kinematic optimization [11] and prototype design [8]. It is characterized by a large workspace free of singularities. The theoretical optimal workspace is as large as 180° of tilting and rocking, and 270° of swivel. The prototype used in the experiments is hydraulically driven by four piston type actuators and achieves 90° of tilting and rocking and 180° of swivel while delivering a torque of nearly 200 N.m throughout its workspace acting on an inertia of the order of 0.01 Kg.m^2. Four LVDT's measure the linear movement of actuators using 12-bit A/D converters. A more complete description of its construction is available in [8].
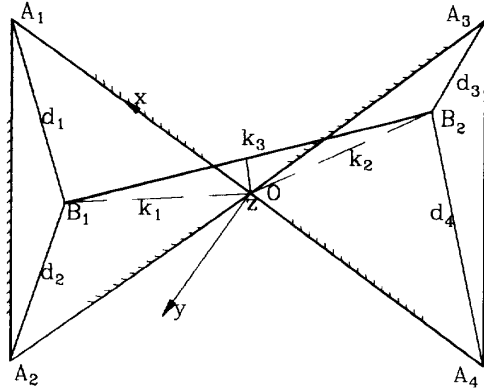
Figure 2: Kinematic model of the shoulder joint viewed from above.

2 Mechanism Kinematics

The kinematic model is shown in Figure 2. A_i (i=1,2,3,4) represents a spherical joint at the stationary side of each actuator. B_1 and B_2 are also spherical and lie in the intersection of the centrelines of each two adjacent actuators. Plane B_1B_2O defines the end plate which should be in the desired orientation. d_i (i=1,2,3,4) is the input of the mechanism and represents a pair of actuator and displacement sensor. k_1 and k_2 are imaginary links which are used in calibration loops.

2.1 Inverse Kinematics

In the inverse kinematics of this robot, d_i (i=1,2,3,4) can be found from the orientation of the end plate pivoted about O. A coordinate frame is chosen in such a way that x is along OA_1, y remains in the plane of A_1A_2O and z is directed out of the paper. So, A_i's are as follows:

$$A_1 = [A_{1x}, 0, 0]^T$$

$$A_2 = [A_{2x}, A_{2y}, 0]^T$$

$$A_3 = [A_{3x}, A_{3y}, A_{3z}]^T \quad (1)$$

$$A_4 = [A_{4x}, A_{4y}, A_{4z}]^T$$

It is to be noted that the above notation is used in the calibration algorithm; in the ideal design, there are some assumptions mentioned in Section 2.2.

From the orientation of the end plate, B_1 and B_2 are found by multiplying the rotation matrix by their initial position vectors. Now, d_i's can be found as follows:

$$d_1 = | B_1 - A_1 |, etc. \quad (2)$$

2.2 Forward Kinematics

In forward kinematics, the orientation of the end plate should be obtained assuming all d_i's are known. Forward kinematics of this manipulator becomes complicated if we do not assume that: a) All A_i's have the same distance from O. b) Points A_2, O, and A_3 are colinear. c) Points A_1, O, and A_4 are colinear. It is fortunate that for our calibration approach, we do not need forward kinematics. Based on the above assumptions, a good solution for the orientation matrix can be found by manipulating (2) [11].

3 Closed-Loop Calibration Procedure

The selection of the parameters to be calibrated is an important issue. In fact, it would be ideal to assume all the kinematic parameters, scale factors (gains) of the sensors, and sensor offsets unknown. But, we should first evaluate the limits of the approach considering measurement errors due to resolution, nonlinearity, and noise of sensors, numerical error of the method used, sensitivity of end plate orientation with respect to change of a parameter, and observability of our parameters. Then, we can decide which parameters should be assumed known and which should be identified.

Length $d_i(k)$ which is measured by the i'th LVDT in the k'th pose is obtained as follows:

$$d_i(k) = S_i * V_i(k) + d_{0i} (i = 1, ..., 4, k = 1, ..., m) \quad (3)$$

where S_i, $V_i(k)$, and d_{0i} represent the gain, output voltage, and offset of the i'th LVDT respectively, and m is the number of measurements. It is worth mentioning that each time LVDT's are disassembled and then reassembled, d_{0i} may change considerably (a few millimeters) and the closed-loop calibration is a promising approach for finding new offsets.

3.1 Least-Square Method

Since the angles are not sensed, the simplest way to formulate calibration equations is to use distance equations. We use measurement redundancy to establish our objective function which is to be minimized. Assume we move the mechanism in m different poses. Define the $4m$-dimensional error vector f with the following components:

$$f(4k - 3) = (B_1^1(k) - A_1)^2 - d_1^2(k)$$

$$f(4k - 2) = (B_1^2(k) - A_2)^2 - d_2^2(k)$$

$$f(4k - 1) = (B_2^3(k) - A_3)^2 - d_3^2(k) \quad (4)$$

$$f(4k) = (B_2^4(k) - A_4)^2 - d_4^2(k)$$

where $k = 1, ..., m$. $d_i(k)$ is obtained by (3). $B_j^i(k)$, $j = 1, 2$ and $i = 1, ..., 4$ is the position vector of point B_j in the k'th pose which is obtained by using measurements of all LVDT's except the i'th one. As an example, let's see how to find $B_2^3(k)$.

We first find $\mathbf{B}_1$ by the intersection of the following three spheres:

Sphere 1: centered at $\mathbf{O}$ with radius k_1,
Sphere 2: centered at $\mathbf{A}_1$ with radius $d_1(k)$,
Sphere 3: centered at $\mathbf{A}_2$ with radius $d_2(k)$.

Then we find $\mathbf{B}_2^3(k)$ by the intersection of the following three spheres:

Sphere 1: centered at $\mathbf{O}$ with radius k_2,
Sphere 2: centered at $\mathbf{A}_4$ with radius $d_4(k)$,
Sphere 3: centered at $\mathbf{B}_1$ (obtained above) with radius k_3.

The objective function to be minimized is defined as:

$$\min_{\mathbf{x}} \mathbf{f}^T \mathbf{f} \qquad (5)$$

The solution is sought by a Gauss-Newton method. It is helpful to find the Jacobian of $\mathbf{f}$ analytically and use it in the least-square method:

$$g(i,j) = \partial f(i)/\partial x(j); i = 1,...,4m; j = 1,...,n. \qquad (6)$$

where $\mathbf{g}$ is Jacobian(gradient), $x(j)$ is the j'th unknown parameter to be calibrated, and n is the number of parameters.

3.2 Scaling

Some inaccuracies in computations are due to ill-conditioning of matrices. In [15] and [2], issues such as scaling, condition number, and the best pose set of the robot for data acquisition in calibration measurement have been discussed.

Scaling is a way to obtain better numerical performance. There are two types of scaling: a) Task Variable Scaling: It is used when the end point position and orientation are to be related to each other to have the same order of precision. In this paper, we do not deal with the combination of orientation and position. b) Parameter Scaling: We normalize the effect of different parameters on the end-effector pose. Column scaling is a way to achieve parameter scaling [12]. The key point is that we normalize the Jacobian to approach the minimum possible condition number. Define a diagonal matrix $\mathbf{H}=\text{diag}(h_1,...,h_n)$ with elements:

$$h_i = \begin{cases} \| \mathbf{g}_i \|^{-1} & if \quad \| \mathbf{g}_i \| \neq 0 \\ 1 & if \quad \| \mathbf{g}_i \| = 0 \end{cases} \qquad (7)$$

where $\mathbf{g}_i$ is the i'th column of $\mathbf{g}$ (Jacobian). Also, we have:

$$\Delta \mathbf{f} = \mathbf{g}\Delta \mathbf{x} = (\mathbf{g}\mathbf{H})(\mathbf{H}^{-1}\Delta \mathbf{x}) = \mathbf{g}\Delta \mathbf{x}$$

$$= \sum_i \frac{\mathbf{g}_i}{\| \mathbf{g}_i \|} \Delta \mathbf{x}_i \| \mathbf{g}_i \| \qquad (8)$$

where $\Delta \mathbf{f}$ is the residual error in the error function, and $\Delta \mathbf{x}$ are the residual parameters. The new Jacobian $\mathbf{g}\mathbf{H}$ has unit column vectors and lower condition number, and our new parameters are multiplied by the norm of the corresponding column of the Jacobian.

3.3 Observability Index

The best pose set of the robot that yields a maximum observability of the parameters must be found. The singular value decomposition yields:

$$\Delta \mathbf{f} = \mathbf{g}\Delta \mathbf{x} = \mathbf{U}\Sigma \mathbf{V}^T \Delta \mathbf{x} \qquad (9)$$

where $\mathbf{U}$ and $\mathbf{V}$ are orthonormal matrices and Σ is a $4m$ by n matrix which is made up of singular values of $\mathbf{g}$ in its main diagonal and zero other elements. It can be shown that [2]:

$$\sigma_L \leq \frac{| \Delta \mathbf{f} |}{| \Delta \mathbf{x} |} \leq \sigma_1 \qquad (10)$$

where σ_L is the smallest singular value of $\mathbf{g}$ and σ_1 is the largest one. It is desired that a very small error in parameters makes the highest possible effect on the sensor measurements. In other words, we look for some pose sets which exhibit the greatest influence of parameter errors (relative to their nominal values) on the objective function. (10) yields:

$$| \Delta \mathbf{f} | \geq \sigma_L | \Delta \mathbf{x} | \qquad (11)$$

i.e. the greater σ_L, the greater $| \Delta \mathbf{f} |$. In fact, we would like to make sure that we achieve the maximum observability of the errors of parameters. So, the observability index is defined as :

$$O = \sigma_L \qquad (12)$$

In [2] the observability index is defined as:

$$O = \frac{\sqrt[L]{\sigma_1...\sigma_L}}{\sqrt{M}} \qquad (13)$$

where L is the number of singular values of $\mathbf{g}$ and M is the number of measurements. A well-known result is that $\sqrt{det(\mathbf{g}^T \mathbf{g})} = \sigma_1...\sigma_L$. So, this observability index (13) is related to the value of the determinant of $\mathbf{g}^T \mathbf{g}$.

Driels and Pathre mentioned that the condition number of the Jacobian $\mathbf{g}$ is an indication of the observability of the parameters to be identified [5]:

$$O = k(\mathbf{g}) = \sigma_1/\sigma_L \qquad (14)$$

where σ_1 is the maximum singular value of $\mathbf{g}$ and σ_L is the minimum. It is to be noted that O in (12) and (13) is to be as large as possible, but in (14), O should be as small as possible.

From a geometrical point of view, we know that if $\Delta \mathbf{x}$ defines a hypersphere in (9), then $\Delta \mathbf{f}$ will be a hyperellipsoid with the shortest semiaxis σ_L and the longest σ_1. Also, the volume of this hyperellipsoid is proportional to the product of singular values of $\mathbf{g}$. (13) conveys the requirement for a big volume, but (12) conveys the idea that the shortest axis should be as long as possible. In other words, in (12) we would like to make sure that our sensor measurements are maximally related to the errors in parameters $(\Delta \mathbf{x})$ while minimizing the influence of noise. In (14) we would like to make the hyperellipsoid close to a hypersphere. In other words, (14) avoids the occurrence

of a sharp hyperellipsoid. It can be shown that a large condition number has a great influence on the amplification of the measurement noise [6]. If we consider the volume of the hyperellipsoid alone, then there is a risk that the measurement corresponding to the smallest hyperellipsoid axis corrupts our results. Now, it is clear that even checking both the condition number (14) and observability index using (13), cannot guarantee the validity of our results.

To compare these observability indices, we assume a hypothetical robot with three parameters which is calibrated by two pose sets A and B. For pose set A, suppose the singular values are:

$$\sigma = \{100, 0.1, 0.1\} \tag{15}$$

and for pose set B:

$$\sigma = \{10, 10, 0.01\} \tag{16}$$

Note that both pose sets have the same condition number. (12) suggests that pose set A yields better observability and (13) treats them the same. It is seen that pose set B may give ten times less observability compared to pose set A.

Finally, we suggest that the smallest singular value along with the condition number should be regarded as the observability indexes.

4 Results

In this section, simulation results are presented, then closed-loop experimental results are presented and are compared to the open-loop results.

4.1 Simulations

In simulation, we considered issues such as: selection of parameters to be calibrated, measurement noise, the required number of robot poses to identify parameters, and the optimum pose set.

4.1.1 Measurement noise

We calibrated each LVDT using the measurement of an accurate milling machine and found that we can find the gain of each LVDT with a noise level of 40mv (or 0.15mm) in the input voltage. Of course, other errors like nonlinearity of the sensors are included in that value, but we treat all sensor errors as noise.

4.1.2 Selection of Parameters to Be Calibrated

As mentioned in section 3, it would be ideal to identify all the robot parameters. We started with these parameters : sensor offsets, sensor gains, A_{1x}, A_{2x}, A_{2y}, A_{3x}, A_{3y}, A_{3z}, A_{4x}, A_{4y}, A_{4z}, k_1, k_2, and k_3. It is to be noted that each time we ran the calibration algorithm, we did column scaling first and then proceeded to the rest of the routine. Some parameters were eliminated through these steps:

a) Inclusion of all the parameters resulted in a high condition number of more than 10000 and erroneous results. On the other hand, we should keep in mind the reliability of our results compared with blue print
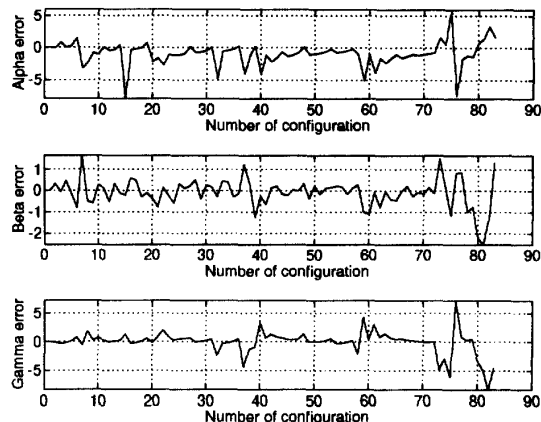

Figure 3: End plate orientation error in degrees due to 1mm error in d_{01}.

data. We should calibrate those parameters which we believe our closed-loop method can detect more accurately than blue print data. Based on manufacturing specifications of the shoulder joint, it is reasonable to assume: $A_{3z} = A_{4z} = A_{4y} = 0$, $A_{3x} = -A_{2x}$, $A_{3y} = -A_{2y}$, $A_{4x} = -A_{1x}$.

b) The calibration routine was very sensitive to the initial guess of scale factors. It was found that we need an accuracy of less than 0.1 percent for the initial guesses. Even in that case, the calibration result was not better than 0.1 percent. In other words, the routine had a tendency to diverge. So, we measured off-line scale factors of each LVDT using the movements of an accurate milling machine. The sensitivity of the nonlinear optimization algorithm to the gains was also reported in [9].

c) We did singular value decomposition of the Jacobian and found that k_3, k_1, and k_2 make the observability index very low. For example, inclusion of k_3 in the routine provided a very low observability index (12) of 0.006, while after removing k_3 as a parameter, observability index rose to 0.1. After elimination of these three parameters, we could get an observability index (12) of 1.8, and condition number of less than 1000. d) We considered the effect of errors of each parameter on the plate orientation. We calibrate those parameters of the robot to which the end plate orientation is more sensitive. To this end, we used Z-Y-Z Euler angles [4] and considered the error produced in α, β, and γ of end plate due to errors in different parameters. Figure 3 shows the change in α, β, and γ due to 1 mm error in d_{01} (offset of the first LVDT). After doing so for all the parameters, we realized that the effects of sensor offsets are as the same order as A_{1x}, A_{2x}, A_{2y}. So, we set the parameters to be calibrated as: sensor offsets, A_{1x}, A_{2x}, and A_{2y}.

Note that because some parameters such as k_3 are

Parameter	Blue print	Open-Loop	Closed-Loop
$d_{01}(mm)$	N/A	97.0	96.8
$d_{02}(mm)$	N/A	100.3	98.8
$d_{03}(mm)$	N/A	95.1	94.6
$d_{04}(mm)$	N/A	100.2	99.6
$A_{1x}(mm)$	68.7	68.3	69.0
$A_{2x}(mm)$	-28.8	-28.9	-28.9
$A_{2y}(mm)$	62.4	62.8	62.2

Table 1: Comparison of calibration results.

known, there is no need to assume a parameter as a reference unit and find other parameters relative to it [1].

4.1.3   Number of Poses

It was found that there is no need to use more than 50 poses to calibrate parameters. These poses are selected as optimal ones, i.e., the observability index (12) (after doing scaling) reaches its maximum value (1.8).

4.2   Closed-Loop Experimental Results

The end plate was moved to different orientations manually and data were acquired simultaneously from four LVDT's through 12-bit A/D converters with a sampling frequency of 20 Hz. 450 poses were recorded. We wrote an algorithm in MATLAB to select 50 poses out of 450 poses to have the maximum observability index (over 1.8) and minimum condition number. Results are shown in Table 1.

4.3   Open-Loop Experimental Results

We carried out an open loop procedure to find the kinematic parameters using an Optotrak 3020 (Northern Digital, Ltd., Waterloo, Ontario) which has a stated accuracy of .1 -.15 mm in a 2.5 m distance. Three IREDs (infrared emitting diodes) were attached to the end plate. The end plate was placed into 100 poses, carefully chosen to be in view of the camera system. At each pose, Optotrak IREDs and LVDT measurements were sampled and averaged 10 times.

A standard iterative least squares method was employed to derive robot parameters, including extra parameters to locate the IREDs in the end plate and also coordinate frame of robot relative to the camera coordinate system. Results are presented in Table 1.

To compare closed-loop and open-loop methods, we consider RMS errors of the three parameters for which we have their nominal values. It turns out that for the closed-loop method, the RMS error is 0.22mm and for the open-loop is 0.33mm. The RMS error of open loop method is a little bit more than that of closed loop method. It can be due to the extra parameters that we had to add in the algorithm to locate IREDs in the end plate and also coordinate frame of robot relative to the camera coordinate system. It also gives us a promising view for the closed-loop method.

5   Discussion

We have presented an autonomous procedure for kinematic calibration of a shoulder joint to identify displacement sensor offsets and 3 other kinematic parameters. This closed-loop procedure requires only the joint displacement sensing, and hence is a viable option for field calibration where end-point measurement is not feasible. This procedure is an extension of an approach initially formulated for single closed kinematic loops [1] to multiple closed loop mechanisms.

Results of simulations and experiments show that the allowable condition number depends on the measurement noise, computer precision, and our desired accuracy. It seemed that condition numbers of up to 1000 are acceptable in the present case.

It was found that our closed loop approach was quite sensitive to sensor gains. If we have some initial guesses which are inaccurate by more than 0.1 percent for the gains, there is a risk of divergence of the algorithm.

It seems that for getting better results, we should also model the compliance of joints and also take into account the possibility of misalignment of intersecting axes.

The observability index was used as a criterion for selection of the best pose set to detect parameter errors. It was shown that the smallest singular value is more reliable for observability index than the product of singular values. In simulation, we used the product of singular values as the observability index, but the RMS of parameter errors did not decrease as the observability index increased. It should be noted that if parameters are of different units (e.g. position and orientation), then the observability index may include different units and the selection of the best pose will be vague. So, the observability index should be considered when the parameters all have the same unit. Generally, to get more accurate and reliable results from the calibration procedure, it is needed that both observability index (12) and condition number be taken into account. One should make an appropriate tradeoff between these two factors based on simulation results.

Similar considerations have been taken into account by others in the field of robot kinematics. Klein and Blaho analyzed some dexterity measures for the design and control of kinematically redundant manipulators[10]. They considered several criteria such as determinant, condition number, and minimum singular value of the Jacobian matrix of manipulator. For redundant manipulators, *manipulability* was defined as:

$$\sqrt{det(\mathbf{g}\mathbf{g}^T)} = \sigma_1 ... \sigma_m \qquad (17)$$

where $\sigma_i (i = 1, ..., m)$ are the singular values of the Jacobian matrix. (17) is similar to (13). It is to be noted that the identification Jacobian in calibration analysis is different from the well-known Jacobian of the manipulators used in (17). They concluded that the minimum singular value has a quantitative interpretation that complements the condition number. They also stated that although in many cases maximizing the

minimum singular value gives the same configuration as minimizing the condition number, in other problems - particularly those with more degrees of freedom - the minimum singular value could be used to choose between cases with equal optimal condition number. Also, it is to be noted that while a determinant going to zero marks the presence of a singularity, the actual value of the determinant cannot be used as a practical measure of the degree of ill-conditioning.

Kurtz and Hayward noticed that the low sensitivity of the condition number made it necessary to consider several measures [11].

Acknowledgments

References

[1] D.J. Bennett and J.M. Hollerbach, "Autonomous calibration of single-loop closed kinematic chains formed by manipulators with passive endpoint constraints," *IEEE Trans. Robotics and Automation*, vol. 7, pp. 597-606, 1991.

[2] J.H. Borm and C.H. Menq, "Determination of optimal measurement configurations for robot calibration based on observability measure," *Intl. J. Robotics Research*, vol. 10, no. 1, pp. 51-63, 1991.

[3] B. Boulet, Modeling and Control of a Robotic Joint with In-Parallel Redundant Actuators, M. Eng. Thesis, McGill University, Dept. Electrical Eng., 1992.

[4] J.J. Craig, *Introduction to Robotics: Mechanics and Control*. Reading, Mass.: Addison-Wesley, 1986.

[5] M.R. Driels and U.S. Pathre, "Significance of Observation Strategy on the Design of Robot Calibration Experiments," *J. of Robotic Systems*, vol. 7, no. 2, pp. 197-223, 1990.

[6] G.H. Golub, and C.F. Van Loan, *Matrix Computations*. Baltimore: Johns Hopkins University Press, 1991.

[7] V. Hayward, R. Kurtz, "Modeling of a parallel wrist mechanism with actuator redundancy," *Advances in Robot Kinematics*, edited by S. Stifter, Lenarcic. Springer-Verlag, pp. 444-456, 1991.

[8] V. Hayward, "Design of a hydraulic robot shoulder mechanism based on a combinatorial mechanism," *Preprints of the Third International Symposium on Experimental Robotics*. Kyoto, Japan:, 1993.

[9] J.M. Hollerbach and D.M. Lokhorst, "Closed-Loop Kinematic Calibration of the RSI 6-DOF Hand Controller," in *IEEE Intl. Conf. Robotics and Automation*, Atlanta, Geogia, pp. 142-148, May 2-6, 1993.

[10] C.A. Klein and B.E. Blaho, "Dexterity measures for the design and control of kinematically redundant manipulators," *Intl. J. Robotics Research*, vol. 6, no. 2, pp. 72-83, 1987.

[11] R. Kurtz and V. Hayward, "Multiple-goal kinematic optimization of a parallel spherical mechanism with actuator redundancy," *IEEE Trans. Robotics and Automation*, vol. 8, pp. 644-651, 1992.

[12] C.L. Lawson and R.J. Hanson, *Solving Least Squares Problems*. Englewood Cliffs, N.J.: Prentice-Hall, pp. 180-198, 1974.

[13] C.H. Menq, J.H. Borm, and J.Z. Lai, "Identification and observability measure of a basis set of error parameters in robot calibration," *J. Mechanisms, Transmissions, and Automation in Design*, vol. 111, pp. 513-518, 1989.

[14] B.W. Mooring, Z.S. Roth, and M.R. Driels, *Fundamentals of Manipulator Calibration*. NY: Wiley Interscience, 1991.

[15] Schroer, K., "Theory of kinematic modelling and numerical procedures for robot calibration," *Robot Calibration*, edited by R. Bernhardt and S.L. Albright. London: Chapman & Hall, pp. 157-196, 1993.

[16] C. Wampler, and T. Arai, "Calibration of robots having kinematic closed loops using non-linear least-squares estimation," in *Proc. IFTOMM Symposium*, Nagoya, Japan, Sept., 1992.

[17] H. Zhuang, B. Li, Z.S. Roth, and X. Xie, "Self-calibration and mirror center offset elimination of a multi-beam laser tracking system," *Robotics and Autonomous Systems*, vol. 9, pp. 255-269, 1992.